JOURNAL OF THE BALKAN GEOPHYSICAL SOCIETY, Vol. 11, No. 1, December 2008, p. 1-9, 10 figs, 3 tables.

2D focusing inversion of gravity data with the use of parameter variation as a stopping criterion

Yunus L. Ekinci

Çanakkale Onsekiz Mart University, Department of Geophysical Engineering, 17020, Çanakkale, Turkey

(ylekinci@comu.edu.tr)

(Received 02 April 2008; accepted 25 September 2008)

Abstract: *A modified 2D focusing inversion method for gravity data is presented in this paper. This iterative inversion method minimizes the area of the causative body and yields a compact density distribution. In order to find the required number of iterations for maximum compactness of the density distribution, the parameter variation function is proposed as a stopping criterion in the inversion procedure. A MATLAB-based inversion code for the proposed method was implemented and was tested on synthetic gravity data. This study revealed that if the causative bodies are compact and have a uniform density contrast, an exact recovery of the compact density distribution can be obtained when the parameter variation reaches a minimum value. Thus, the parameter variation function determines the required number of iterations for 2D focusing inversion of the gravity data.*

Key words: *Gravity, 2D Inversion, Focusing, Maximum Compactness, Stopping Criterion, Parameter Variation*

INTRODUCTION

Potential field data are usually analyzed by employing linear transformations, spectral methods, inversion techniques and analytic signal methods. The analytic signal methods usually combine the horizontal and vertical gradients of the gravity or magnetic field in order to define the edges of the body (e.g. Roest, et al., 1992; Roest and Pilkington, 1993; Debeglia and Corpel, 1997; Bilim and Ateş, 2003). Linear transformations facilitate the geologic interpretations. They provide insights about the nature of the sources (Blakely, 1995). The most commonly used transformations are upward and downward continuations, reduction to the pole, gravity to magnetic fields conversion and vice versa (e.g. Gunn, 1975; Gilbert and Galdeano, 1985; Stavrev and Gerovska, 2000; Büyüksaraç, et al., 2005).

Spectral methods use the energy spectrum of the anomalies to determine the mean depth of rectangular block ensembles or prismatic bodies (e.g. Spector and Grant, 1970; Okubo, et al., 1985; Dolmaz, et al., 2005; Gelişli and Maden, 2006). On the other hand, the inversion methods determine the parameters of the model, whose response is similar to observed data. Unfortunately the non-uniqueness problem is more pronounced in the inversion of potential field data. Namely, according to Gauss theorem, if the field is known only on a bounding surface, there are infinitely many equivalent source distributions inside the boundary that can produce this field (Li and Oldenburg, 1996). A common way of overcoming this problem is to add a priori information to constrain the solution. Many relevant studies can be found in the literature: Green (1975) chose to minimize a weighted model norm with respect to a reference model in an effort to guide the inversion according to the available information. Last and Kubik (1983) used a compact solution with a minimum volume constraint. Barbosa and Silva (1994) concentrated the solution along inertial axes, while Li and Oldenburg (1996, 1998) reduced the effect of the decreasing sensitivity of blocks with depth by weighting them appropriately. Boulanger and Chouteau (2001) proposed minimum distance, flatness, smoothness and compactness constraints for the inversion of gravity data, which are combined using a Lagrangian formulation. Li and Oldenburg (2003) used wavelet transforms and a logarithmic barrier method for the inversion of large magnetic data sets.

Within the context of this study, the 2D inversion method proposed by Last and Kubik (1983) is revisited. For this purpose a MATLAB-based 2D inversion code was developed. This code uses an iterative least squares procedure, which allows the weights to depend on the densities of the previous iteration. Therefore, the solution minimizes both the area of the body and a weighted sum of squared residuals (Blakely, 1995).

In practice, the inversion procedure terminates when the misfit between the observed data and the synthetic data produced by the obtained model reaches a chosen value. This stopping criterion often does not provide satisfactory solutions when the inversion problem of potential field data is underdetermined. In such cases, the parameter variation function is proposed as an alternative. This function is computed using the parameters at successive iterations.

ANOMALY OF A 2D DENSITY DISTRIBUTION

In order to calculate the anomaly of a 2D density distribution, a rectangular grid is employed. In this 2D model the density varies both laterally and vertically. Let the xz coordinates be chosen such that x-axis is parallel to the ground surface and the z-axis points vertically downwards. Let the subsurface be divided into rectangular blocks, whose side along x-axis is equal to the distance between two observation points. Then, for the 2D model, shown in Figure 1, the gravity effect of all the rectangular blocks at the observation point *i*, is given by:

$$g_i = \sum_{j=1}^{M} \alpha_{ij} v_j \quad i = 1.....N, \tag{1}$$

where M denotes the number of blocks, N, the numbers of observations, v_j is the density of the jth block and α_{ij} matrix element representing the influence of the jth block on the ith gravity value. In order to calculate the matrix element α_{ij} one can employ the following equation (Blakely, 1995):

$$g = \gamma v \sum_{n=1}^{L} \frac{\beta_n}{1 - \alpha_n^2} \left[\log \frac{r_{n+1}}{r_n} - \alpha_n \left(\Theta_{n+1} - \Theta_n \right) \right] \tag{2}$$

which provides the vertical gravitational attraction due to a 2D prism of polygonal cross section. L denotes the number of sides of the polygon, r_n, r_{n+1}, Θ_n and Θ_{n+1} are defined in Figure 1 for the upper side of a square block, while α_n and β_n are given from the equations:

$$\alpha_n = \frac{x_{n+1} - x_n}{z_{n+1} - z_n} \qquad \beta_n = x_n - \alpha_n z_n \tag{3}$$

Here, z_n and z_{n+1} denote the z coordinate of the two end points of side n and x_n, x_{n+1}, the corresponding x coordinate.

This general formulation is here implemented for rectangular blocks. Thus, the gravity effect of all blocks at every observation point can be easily calculated. The equation (1) which calculates the gravity anomaly can be written in matrix notation as:

$$[G] = [A].[V] \tag{4}$$

where the vector G denotes the observed gravity data, the vector V describes the density distribution and A is the Jacobian matrix whose elements are calculated by equation (2). Figure 2 shows the elements of the Jacobian matrix for 13 observations derived from a homogeneous model represented by a 4 x 13 blocks, having the dimensions of 10 x 10 m.

OUTLINE OF THE INVERSION PROCEDURE

Last and Kubik (1983) proposed an inversion method which provides compact and structurally simple gravity models. This method requires the minimization of a suitable functional of the densities. More specifically they proposed the following functional:

$$q = \sum_{j=1}^{M} w_{vj} {v_j}^2 \rightarrow minimum \tag{5}$$

where the density weighting function is given by:

$$W_{vj} = (v_j^2 + \beta)^{-1} \tag{6}$$

and β is a small number. Here, this method is revisited using the more compact notation for the forward problem. The classical weighted least squares solution is given by:

$$V = W_v^{-1} A^T (A W_v^{-1} A^T)^{-1} G \tag{7}$$

In fact an iterative procedure is followed where the density dependent weights are given by equation (6). At the mth step, the density distribution can be given by:

$$V^{(m)} = \left[({W_v}^{m-1})^{-1} A^T (A \ ({W_v}^{m-1})^{-1} A^T)^{-1} \right] G \tag{8}$$

where the weighting function is defined by the outcome of the previous iteration as follows:

$$\left[W_v^{m-1}\right]_{jj} = \left(\left[v_j^{m-1}\right]^2 + \beta\right)^{-1} \quad (9)$$

Initially the weighting matrix is set to be the identity matrix. Hence, the procedure starts from the least squares solution. Next, the weighting function is calculated and is used in the least squares inversion in order to increase the compactness of the model. According to Last and Kubik (1983) the iterative procedure stops when a minimum area of the density distribution is reached.

The stopping criteria in inversion algorithms are usually based on the fit between the observed data and theoretical data produced by the proposed model. Typical fit or misfit estimators are the following:

$$Misfit = \frac{\left(\sum_{i=1}^{N}\left(d_i^{obs} - d_i^{cal}\right)^2\right)^{1/2}}{\left(\sum_{i=1}^{N}\left(d_i^{obs}\right)^2\right)^{1/2}}$$

$$rms = \frac{\left(\sum_{i=1}^{N}\left(d_i^{obs} - d_i^{cal}\right)^2\right)^{1/2}}{N} \quad (10)$$

where the superscript "*obs*", denotes observed and the superscript "*cal*", calculated data.

In the inversion of potential field data, the number of observations is often less than the number of unknowns (underdetermined problem). To overcome this problem, I introduce an additional criterion, namely the parameter variation function. This criterion was tested using synthetic data. If k is the iteration number and v is the block density vector, the parameter variation function is:

$$smy = \left(\sum_{i=1}^{M}\left(v_i^k - v_i^{k-1}\right)^2\right)^{1/2} \quad (11)$$

The focusing inversion method proposed by Last and Kubik (1983) was modified in order to produce a compact final model. For this model, the difference between the block densities at the last successive iteration is minimum.

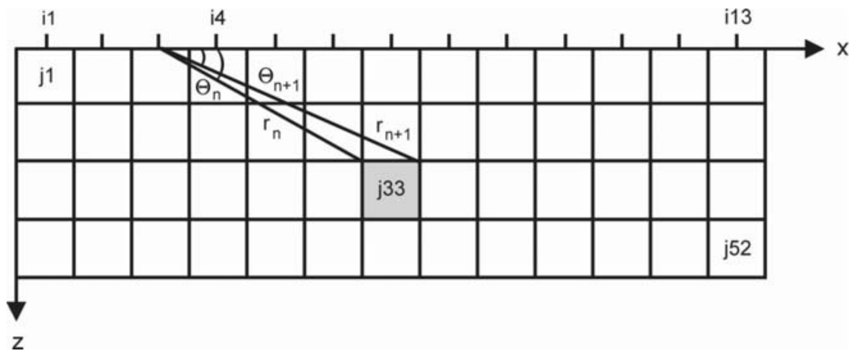

FIG. 1. The 2D subsurface model showing the data points (i) and the constant density blocks (j).

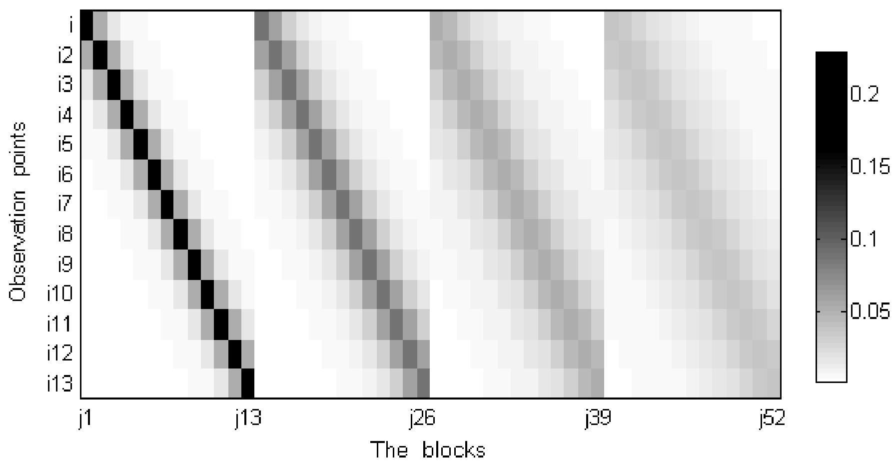

FIG. 2. Amplitude of the Jacobian matrix with respect to observation points and the blocks.

THEORETICAL EXAMPLES

The modified inversion method is tested using three simple examples. At the first example the subsurface is represented by 4 x 13 blocks, having the dimensions of 10 x 10 m. The 2D body is formed by 6 blocks and the density contrast is 2.5 g/cm^3. The 2D body and its gravity anomaly are shown in Figure 3. During the inversion process the density distribution was spread to all the blocks at the first iteration, while at the following iterations the density of the causative blocks increased and the density of the other blocks decreased. The misfit is very small close to zero (Fig. 4) but it is not converge. Thus the misfit can not be used as a stopping criterion. On the other hand the parameter variation gradually reached a minimum after the 8th iteration (Fig. 5). According to the density distribution given on Table 1, the original density distribution has been recovered.

The causative body and associated anomaly for the second example are shown in Figure 6. The density contrast is set to 1 g/cm^3 for the causative body. The blocks dimensions are 10 x 10 m. The parameter variation exhibits similar response (Fig. 7) for this more complex 2D body. The density distribution after the 1st, 4th and 7th iterations is given on Table 2.

In the last example there are three distinct bodies whose density contrast is 1 g/cm^3, 2 g/cm^3 and 3 g/cm^3 respectively (Fig. 8). The subsurface is represented by 3 x 13 blocks, having the dimensions of 10 x 10 m. The inversion method performed equally well in this case. In particular the parameter variation function reached a minimum after the 11th iteration (Fig. 9). According to Table 3, initially all the blocks have nonzero densities. At the 10th iteration only 6 blocks exhibit nonzero density contrast (Fig. 10).

These synthetic examples indicate that the maximum compactness algorithm increases the density of some blocks and decreases the density of the rest. Last and Kubik proposed another constraint on densities namely $v_j/b \leq 1$, j=1,2,…m. According to this constraint for blocks whose density exceeds the limit b, their density is set equal to this value. Here, the density limits were set to $0 < \nu < 2.5$ g/cm^3 for the first example and the inversion procedure converged faster to the satisfactory solutions (not presented). Moreover, these tests showed that the success of the algorithm strongly depends on the selection of the β value. More specifically, $\beta = 10^{-8}$ gives satisfactory results without causing numerical instability.

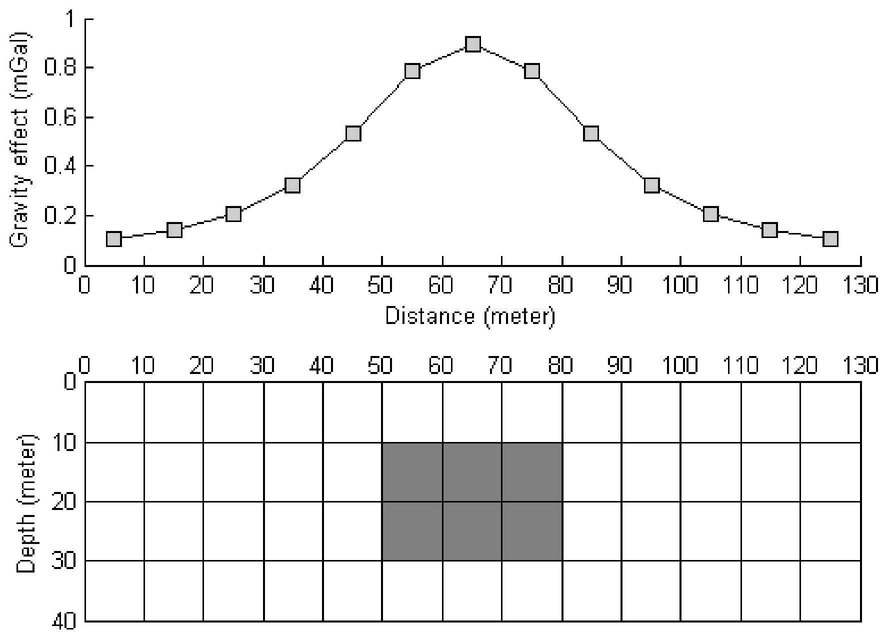

FIG. 3. The causative body and the gravity data for Model 1.

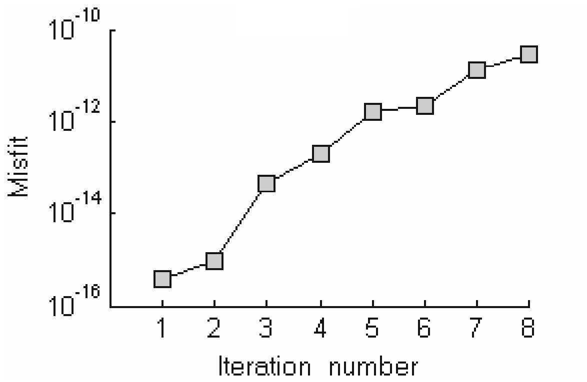

FIG. 4. Misfit values against the iteration number for Model 1.

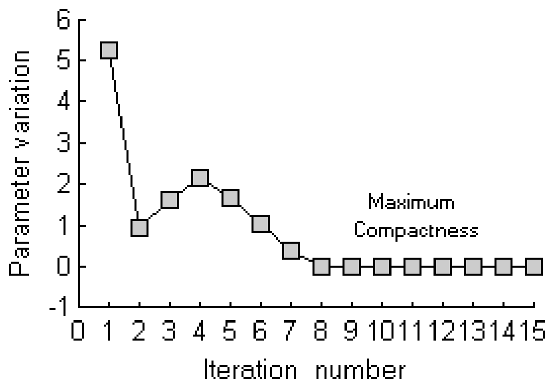

FIG. 5. Parameter variation values against the iteration number for Model 1.

Table 1. Block densities for Model 1.

1st iteration (g/cm^3)												
-0.06	-0.07	-0.06	0.03	0.43	1.17	1.46	1.17	0.43	0.03	-0.06	-0.07	-0.06
0.01	0.03	0.08	0.21	0.46	0.75	0.88	0.75	0.46	0.21	0.08	0.03	0.01
0.06	0.09	0.15	0.26	0.40	0.53	0.59	0.53	0.40	0.26	0.15	0.09	0.06
0.09	0.12	0.18	0.25	0.33	0.40	0.43	0.40	0.33	0.25	0.18	0.12	0.09
5th iteration (g/cm^3)												
				0.04	2.67	2.56	2.67	0.04				
				0.17	1.65	2.91	1.65	0.17				
				0.02	0.12	0.19	0.12	0.02				
7th iteration (g/cm^3)												
					2.50	2.50	2.50					
					2.50	2.50	2.50					

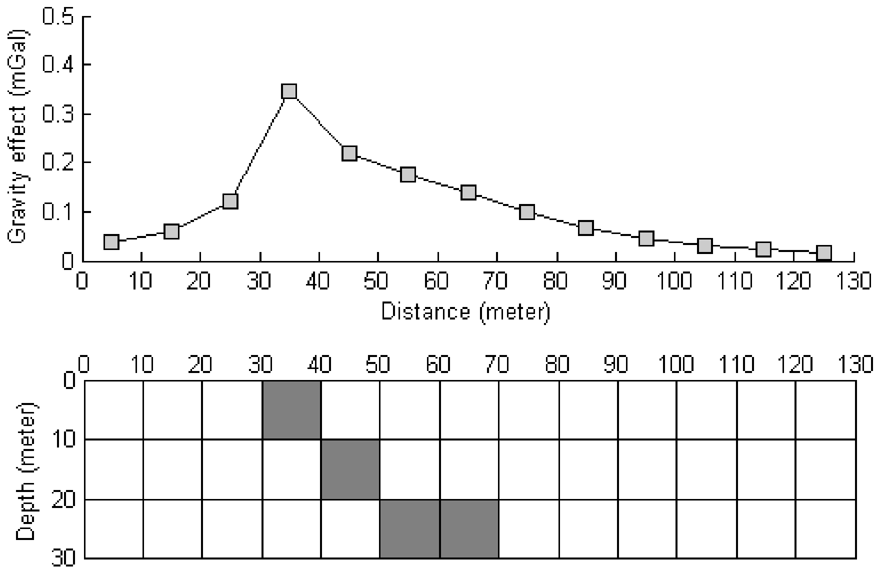

FIG. 6. The causative body and the gravity data for Model 2.

FIG. 7. Parameter variation values against the iteration number for Model 2.

Table 2. Block densities for Model 2.

1st iteration (g/cm³)												
-0.04	-0.06	-0.08	1.00	0.21	0.19	0.14	0.08	0.03	0.00	-0.00	-0.00	-0.00
0.01	0.04	0.16	0.33	0.27	0.18	0.13	0.09	0.05	0.03	0.02	0.01	0.01
0.04	0.08	0.14	0.19	0.19	0.16	0.12	0.09	0.06	0.04	0.03	0.02	0.02
4th iteration (g/cm³)												
			1.02	0.05	0.01							
				0.70	0.27	0.15	0.06					
			0.05	0.47	0.58	0.39	0.17	0.04	0.01			0.01
7th iteration (g/cm³)												
			1.00									
				1.00								
					1.00	1.00						

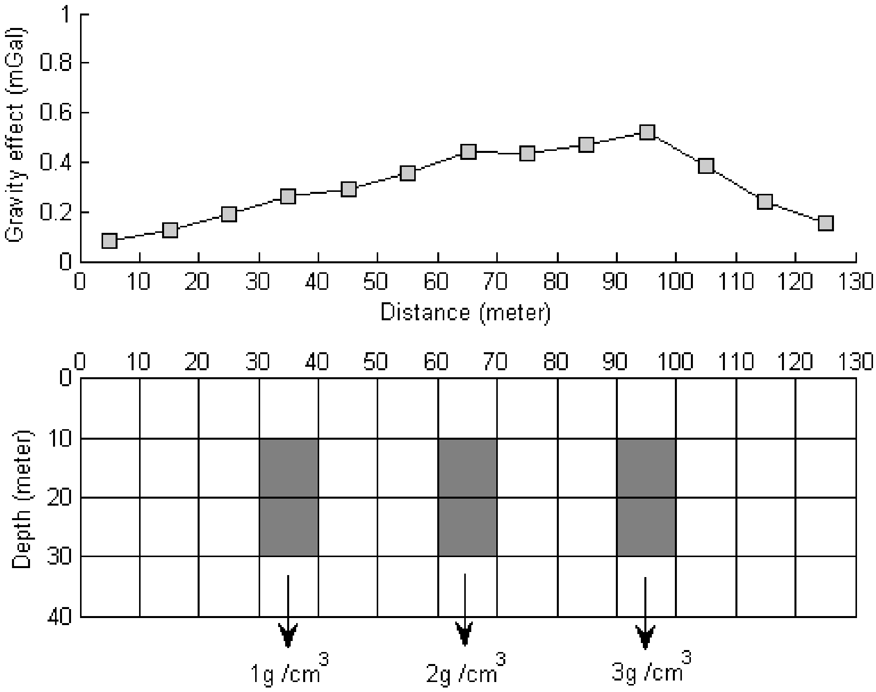

FIG. 8. The causative bodies and the gravity data for Model 3.

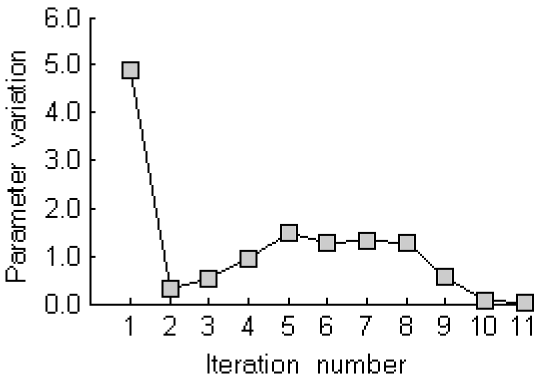

FIG. 9. Parameter variation values against the iteration number for Model 3.

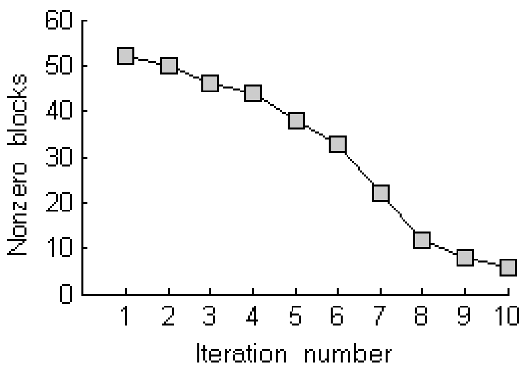

FIG. 10. The number of the nonzero density blocks against iteration number.

Table 3. Block densities for Model 3.

1^{st} iteration (g/cm^3)												
-0.03	-0.01	0.11	0.26	0.17	0.29	0.56	0.37	0.49	0.86	0.42	0.06	-0.02
0.03	0.06	0.12	0.18	0.22	0.29	0.37	0.39	0.43	0.46	0.34	0.18	0.09
0.06	0.09	0.13	0.17	0.21	0.26	0.30	0.33	0.34	0.33	0.27	0.19	0.12
0.07	0.10	0.13	0.16	0.19	0.22	0.25	0.27	0.28	0.26	0.23	0.18	0.14
6^{th} iteration (g/cm^3)												
		0.01	0.04		0.01	0.07		0.01		0.01		
		0.04	0.86	0.01	0.19	1.73	0.25	0.01	3.34	0.01	0.02	
		0.15	0.55	0.35	0.50	0.67	0.47	0.60	1.25	0.59	0.03	
			0.02	0.04	0.06	0.05	0.04	0.03	0.02			
10^{th} iteration (g/cm^3)												
			1.00			2.00			3.00			
			1.00			2.00			3.00			

CONCLUSIONS

A MATLAB-based algorithm proposed by Last and Kubik (1983) was developed based on 2D focusing inversion of gravity data. A parameter variation function as a stopping criterion was proposed and tested on the synthetic examples. Searching for the minimum of the parameter variation function proved useful for the inversion of error free gravity data. The use of parameter variation criterion improves the focusing inversion process for compact causative bodies which exhibit a uniform density contrast. Additional tests must be done using noisy synthetic or real data.

Provided that the lower and upper limits of the density distribution are chosen properly, this modified focusing inversion technique converges faster to the satisfactory solutions. This algorithm can easily be modified for the inversion of magnetic data.

ACKNOWLEDGMENTS

I would like to express my gratitude to Dr. Emin U. Ulugergerli for his valuable suggestions. Prof. Gregory N. Tsokas and the other anonymous reviewer are thanked for their useful criticism that helped to improve the paper.

REFERENCES

Barbosa, V.C.F., and Silva, J.B.C., 1994, Generalized compact gravity inversion: Geophysics, 59 (1), 57-68.

Bilim, F., and Ateş, A., 2003, Analytic signal inferred from reduced to the pole data: Journal of the Balkan Geophysical Society, 6 (2), 66-74.

Blakely, R.J., 1995, Potential Theory in Gravity and Magnetic Applications: Cambridge University Press.

Boulanger, O., and Chouteau, M., 2001, Constraints in 3D gravity inversion: Geophysical Prospecting, 49 (2), 265-280.

Büyüksaraç, A., Jordanova, D., Ateş, A., and Karloukovski, V., 2005, Interpretation of the gravity and magnetic anomalies of the Cappadocia region, Central Turkey: Pure and Applied Geophysics, 162 (11), 2197-2213.

Debeglia, N., and Corpel, J., 1997, Automatic 3-D interpretation of potential field data using analytic signal derivatives: Geophysics, 62 (1), 87-96.

Dolmaz, M.,N., Hisarlı, Z.M., Ustaömer, T., and Orbay, N., 2005, Curie point depths based on spectrum analysis of aeromagnetic data, West Anatolian extensional province, Turkey: Pure and Applied Geophysics, 162 (3), 571-590.

Gelişli, K., and Maden, N., 2006, Analysis of potential field anomalies in Pasinler-Horasan basin, Eastern Turkey: Journal of the Balkan Geophysical Society, 9 (1), 1-7.

Gilbert, D., and Galdeano, A., 1985, A computer program to perform transformations of gravimetric and aeromagnetic surveys: Computers and Geosciences, 11 (5), 553-588.

Green, W.R., 1975, Inversion of gravity profiles by use of a Backus-Gilbert approach: Geophysics, 40 (5), 763-772.

Gunn, P.J., 1975, Linear transformations of gravity and magnetic fields: Geophysical Prospecting, 23 (2), 300-312.

Last, B.J., and Kubik, K., 1983, Compact gravity inversion: Geophysics, 48 (6), 713–721.

Li, Y.G., and Oldenburg, D.W., 1996, 3-D inversion of magnetic data: Geophysics, 61 (2), 394–408.

Li, Y.G., and Oldenburg, D.W., 1998, 3-D inversion of gravity data: Geophysics, 63 (1), 109–119.

Li, Y.G., and Oldenburg, D.W., 2003, Fast inversion of large scale magnetic data using wavelet transforms and a logarithmic barrier method: Geophysical Journal International, 152 (2), 251-265.

Okubo, Y., Graf, J. R., Hansen, R. O., Ogawa, K., and Tsu, H., 1985, Curie point depths of the Island of Kyushu and surrounding areas, Japan: Geophysics, 50 (3), 481–494.

Roest, W.R., Werhoef, J., and Pilkington, M., 1992, Magnetic interpretation using the 3-D analytic signal: Geophysics, 57 (1), 116-125.

Roest, W.R., and Pilkington, M., 1993, Identifying remanent magnetization effects in magnetic data: Geophysics, 58 (5), 653-659.

Spector, A., and Grant, F.S., 1970, Statistical models for interpreting aeromagnetic data: Geophysics, 35 (2), 293–302, 1970.

Stavrev, P., and Gerovska, D., 2000, Magnetic field transforms with low sensitivity to the direction of source magnetization and high centricity: Geophysical Prospecting, 48 (2), 317-340.